Reactive oxygen species mediated oxidative stress links diabetes and atrial fibrillation

XUE LIANG[*], QITONG ZHANG[*], XINGHUA WANG, MENG YUAN, YUE ZHANG, ZHAO XU, GUANGPING LI and TONG LIU

Tianjin Key Laboratory of Ionic-Molecular Function of Cardiovascular Disease, Department of Cardiology, Tianjin Institute of Cardiology, Second Hospital of Tianjin Medical University, Tianjin 300211, P.R. China

Abstract. Diabetes is an independent risk factor for atrial fibrillation (AF); however, the underlying mechanism linking diabetes and AF remains to be clarified. The present study aimed to explore the molecular mechanism of increased reactive oxygen species (ROS) production in AF and the ROS-mediated downstream events in diabetes. Firstly, the atrial fibroblasts were isolated from the left atrium of rabbits using enzyme digestion and differential adhesion. Then, the isolated cells were identified by morphology analysis under a microscope, collagen distribution using Masson trichrome staining and vimentin by immunofluorescence. Following this, the collected atrial fibroblasts were randomly divided into 7 groups and administered with high glucose (25 mM glucose), H_2O_2 stimulation (100 nmol/l), glucose + apocynin (100 μg/ml), H_2O_2 + apocynin, glucose + H_2O_2, and a combination of glucose, apocynin and H_2O_2, as well as the negative control (NC). An MTS assay was performed to investigate cell proliferation following the different treatments, and western blotting was conducted to explore the expression of several proteins including NAD(P)H oxidative (NOX) subunits, key factors involved in mitogen-activated protein kinase (MAPK) signaling pathways and matrix metalloproteinases (MMPs). The atrial fibroblasts were spindle-shaped with one or more protuberances. Vimentin was positively expressed in collected cells under confocal laser scanning microscopy. This result indicated that the atrial fibroblasts were successfully prepared. High glucose and H_2O_2 stimulation significantly increased the proliferation of atrial fibroblasts and apocynin markedly attenuated the promoting effects on cell proliferation induced by high glucose and H_2O_2 treatment (P<0.05). Additionally, high glucose and H_2O_2 stimulation increased the expression of Rac1, phospho(p)-c-Jun N-terminal kinase 1, p38, p-p38 and MMP9, which was markedly decreased by the addition of apocynin (P<0.05). The mechanism associated with diabetes and AF may be attributed to oxidative stress (ROS production) derived from NOX activity, and then induced activation of the MAPK signaling pathways and MMP9 expression.

Introduction

Atrial fibrillation (AF) is the most common cardiac arrhythmia, which is characterized by rapid, irregular electrical and mechanical activation of the atria, leading to uncoordinated contraction and atrial thrombi formation (1). AF has become an increasing health-care burden; there is an increased risk of mortality and morbidity in patients with AF, primarily due to stroke and heart failure, resulting in disability and large health-care costs (2). The incidence of AF increases with age (3,4). In addition, several factors have been demonstrated to be associated with the development of AF, including the presence of ischemic heart disease, hypertension, diabetes, cardio-pulmonary diseases and heavy alcohol consumption (5,6). Furthermore, AF is a common postoperative complication, particularly in patents following cardiothoracic surgery (7).

AF pathogenesis is very complex and multifactorial, and the detailed molecular mechanism underlying AF development is still unidentified. Beneficial efficacy has been reported for current drugs used to treat AF, which primarily act by blocking β-adrenergic receptors or ion channels; however, limited long-term efficacy has been identified (8,9). Thus, better understanding of the underlying molecular mechanism is essential for developing novel therapeutic strategies for AF. Previous studies indicated that atrial electrical remodeling and structural remodeling are the pathological basis for AF generation and maintenance (10,11). In addition, it is well accepted that inflammation and oxidative stress serve an important role in the development of AF (10,11).

Oxidase stress refers to the imbalance of pro-oxidants and antioxidants *in vivo*, shifting the balance towards pro-oxidants. An excess of reactive oxygen species (ROS) can directly

Correspondence to: Professor Tong Liu, Tianjin Key Laboratory of Ionic-Molecular Function of Cardiovascular Disease, Department of Cardiology, Tianjin Institute of Cardiology, Second Hospital of Tianjin Medical University, 23 Pingjiang Road, Hexi, Tianjin 300211, P.R. China
E-mail: liutongdoc@126.com

[*]Contributed equally

cause myocardial apoptosis and fibrosis (10). In addition, the increased level of ROS, including superoxide and H_2O_2, has been observed to be associated with AF development (12-14). Increased levels of ROS also induce proteins, lipids and DNA damage, and promotes inflammation by stimulating inflammatory factor secretion from activated inflammatory cells (15,16). Furthermore, ROS has been reported to be involved in cardiac electrical and structural remodeling (17,18). The promoting effects of ROS on inflammation and cardiac remodeling increase susceptibility to AF. Antioxidants that are capable of reducing peroxidation can reverse cardiac structural remodeling and fibrosis (19). However, the molecular mechanism of increased ROS production in AF and the ROS-mediated downstream events have not been defined. NAD(P)H oxidases (NOXs) are a major initiating source for increased ROS production in cardiovascular diseases. The present study will discuss its role in AF development.

Additionally, diabetes is an independent risk factor for AF (20,21), and the mechanism underlying AF development induced by diabetes may be associated with oxidase stress (excess ROS) and inflammation (22,23). Therefore, the present study was performed to explore the molecular mechanism of increased ROS production and ROS-mediated downstream events in AF induced by diabetes.

Materials and methods

Isolation and cultivation of atrial fibroblasts. The present study obtained experimental animal use approval from the Experimental Animal Administration Committee of Tianjin Medical University and Tianjin Municipal Commission for Experimental Animal Control (Tianjin, China), following the guidelines established by the U.S. National Institutes of Health (https://grants.nih.gov/grants/olaw/guide-for-the-care-and-use-of-laboratory-animals.pdf).

Male New Zealand rabbits at 3-4 months old (n=60; weight, 1.5-2.0 kg) provided by Tianjin Institute of Cardiology (Tianjin, China) were used in the present study. Rabbits were housed in a specific pathogen-free animal room maintained at 25˚C, 60% humidity and on a 12-h light/dark cycle with free access to food and water prior to experiments. Primarily, the rabbits were anesthetized with an intravenous injection of ketamine (75 mg/kg) and xylazine (0.75 mg/kg) and then sacrificed with a lethal dose of thiopental (35 mg/kg). Hearts were removed via median thoracotomy and immediately immersed in precooled phosphate-buffered saline (PBS; Wuhan Boster Biological Technology, Ltd., Wuhan, China) containing penicillin (100 U/ml) and streptomycin (100 μg/ml). Subsequently, the epicardium and adipose tissue were cut using eye scissors and the tissues of the left atrium were cut into 1 mm³ patches. These patches were rinsed with PBS until the red blood cells were removed. Then atrial tissue samples were subjected to enzymatic digestion (0.25% trypsin) at 37˚C under agitation (60 rpm) for 10 min and dispersed by gentle trituration with a pipette. The supernatant was collected and mixed with 2 ml Dulbecco's modified Eagle's medium (DMEM; Cellgro; Corning Inc., Corning, NY, USA) containing 4 mM glucose. The mixture was centrifuged at 600 x g for 4 min at room temperature to precipitate cells. Then cells were suspended with PBS and perfused with 0.1% collagenase II

for 10 min. DMEM containing 10% fetal bovine serum (FBS; Junyao Biotechnology Co., Ltd., Beijing, China) was added to the mixture to terminate digestion and centrifugation was performed at 500 x g for 5 min at room temperature to pellet the cells. The harvested cells were collected in DMEM containing 10% FBS and incubated in an incubator with 37˚C and 5% CO_2 for 60-90 min. Following this, the adherent cells were harvested and incubated in DMEM containing 20% FBS and 4 mM glucose at 37˚C and 5% CO_2. Cells were passaged three times.

Identification of atrial fibroblasts by Masson trichrome staining. The cultured cells were placed on slides and fixed in 4% formaldehyde at room temperature for 15 min. Following three washes with DMEM, cells were stained in hematoxylin solution at room temperature for 5 min. Excess dye was removed with hydrochloric acid in ethanol and then cells were stained with Ponceau-acid fuchsin at room temperature for 10 min. Cells were immersed in 2% glacial acetic acid solution, followed by 1% phosphomolybdic acid solution (Sigma-Aldrich; Merck KGaA, Darmstadt, Germany). Without washing, cells were directly stained with aniline blue at room temperature for 5 min. Excess dye was removed with phosphomolybdic acid solution (1%) and glacial acetic acid solution (1%). Finally, cells were dehydrated by an alcohol gradient, washed with xylene and then sealed with neutral gum.

Identification of vimentin by immunofluorescence. The cultured slides of atrial fibroblasts (1x10⁶/ml) were transferred to 6-well plates and washed with cold PBS solution for 5 min. Then slides were treated with 4% formaldehyde for fixation at 4˚C for 15 min and permeated with 2% Triton X-100 in PBS solution at 4˚C for 20 min. Following washing with PBS solution containing 0.25% Triton X-100, slides were blocked with PBS containing 5% bovine serum albumin (Sigma-Aldrich; Merck KGaA) and 0.5% sheep serum albumin solution (BD Biosciences, Franklin Lakes, NJ, CA, USA) for 4 h. Subsequently, slides were incubated with mouse anti-vimentin antibodies (ab28028; Abcam, Cambridge, MA, USA) diluted to 1:500 at 4˚C overnight, followed by horseradish peroxidase (HRP)-conjugated goat anti mouse IgG (ab205719; Abcam) diluted to 1:1,000 for 1 h at room temperature. Slides were counterstained with 4'6-diamidino-2-phenylindole for 10 min at room temperature and 10 random fields were viewed using a confocal laser scanning microscope.

Treatments in atrial fibroblasts. The cultured atrial fibroblasts were randomly divided into seven groups and treated as follows: i) NC group, cells were cultured in DMEM medium containing 4 mM glucose without any treatment; ii) Glu group, cells were cultured in DMEM medium containing 25 mM glucose without other treatment; iii) Glu+Apo group, cells were cultured in DMEM medium containing 25 mM glucose and 100 μg/ml apocynin (Sigma-Aldrich; Merck KGaA); iv) H_2O_2 group, cells were cultured in DMEM medium containing 4 mM glucose and treated with 100 nmol/l H_2O_2; v) H_2O_2+Apo group, cells were cultured in DMEM medium containing 4 mM glucose and 100 μg/ml apocynin, and treated with 100 nmol/l H_2O_2; vi) Glu+H_2O_2 group, cells were

cultured in DMEM medium containing 25 mM glucose and treated with 100 nmol/l H_2O_2; vii) Glu+H_2O_2+Apo group, cells were cultured in DMEM medium containing 25 mM glucose and 100 μg/ml apocynin, and treated with 100 nmol/l H_2O_2.

Detection of cell proliferation by MTS assay. The cultured atrial fibroblasts (3,000/well) following the different treatments were placed in 96-well plates and detected for cell proliferation following incubation for 1, 3 and 5 days by MTS assay (Promega Corp., Madison, WI, USA). Briefly, 100 μl DMEM containing 20% MTS solution was added to each well of the 96-well plates, which were then incubated in an incubator with 37°C and 5% CO_2 for 2 h. The optical density (OD) was then read at 490 nm with a microplate spectrophotometer (BioTek Instruments, Inc., Winooski, VT, USA). Cell proliferation was evaluated according to the standard curve of OD value, which was plotted based on different cell densities (0, $1x10^3$, $3x10^3$, $5x10^3$, $1x10^4$ and $2x10^4$/well).

Western blot analysis. Following 72 h incubation, atrial fibroblasts were washed with precooled PBS and lysed in radioimmunoprecipitation assay buffer (150 mM NaCl, 1% Nonidet P40, 0.5% deoxysodium cholate, 0.1% SDS and 50 mM Tris-HCl) solution containing 10 μl protease inhibitor cocktail (Sigma-Aldrich; Merck KGaA) for 20 min on ice. The lysates were separated by centrifugation at 4°C and 600 x g for 20 min and the supernatant was collected. Total protein concentration was evaluated using a bicinchoninic acid assay kit (Pierce; Thermo Fisher Scientific, Inc., Waltham, MA, USA). Following this, protein samples (30 μg) were separated by 8-14% SDS-PAGE and transferred onto polyvinylidene fluoride membranes (EMD Millipore, Billerica, MA, USA). Then membranes were blocked in 5% non-fat milk in TBS with 0.05% Tween-20 (TBST) at room temperature for 2 h. Following washing with TBST three times, membranes were incubated with mouse anti-extracellular signal-regulated kinase 1 (Erk1; ab32537; 1:1,000; Abcam), phospho-Erk1 (ab131438; 1:1,000), Ras-related C3 botulinum toxin substrate 1 precursor (Rac1; ab33186; 1:1,000), phospho-p38 (ab4822; 1:1,000), phospho-c-Jun N-terminal kinase 1 (Jnk1; ab47337; 1:1,000), p22phox (ab75941; 1:1,000), matrix metalloproteinase 2 (MMP2; ab2462; 1:1,000), MMP9 (ab58803; 1:500), gp91phox (ab80508; 1:1,000), Jnk1 (ab213521; 1:1,000), p38 (ab-31828; 1:1,000) and β-actin (ab8226; 1:10,000) antibodies at 4°C overnight, followed by incubation with HRP-labeled secondary antibodies (ab205719; 1:10,000; all from Abcam) at room temperature for 2 h. Finally, membranes were washed with TBST and visualized by enhanced chemiluminescence reagents and the Chemi-Doc imaging system (Bio-Rad Laboratories, Inc., Hercules, CA, USA). The expression of specific protein was quantified by the grey value normalized to β-actin using TotalLab software version 1.11 (Ultra-Lum Inc., Claremont, CA, USA).

Statistical analysis. In the present study, data were presented as the mean ± standard deviation and subjected to a one-way analysis of variance followed by Duncan's multiple range test. P<0.05 was considered to indicate a statistically significantly difference. All statistical analysis was performed using SPSS software (version 21.0; IBM SPSS, Armonk, NY, USA).
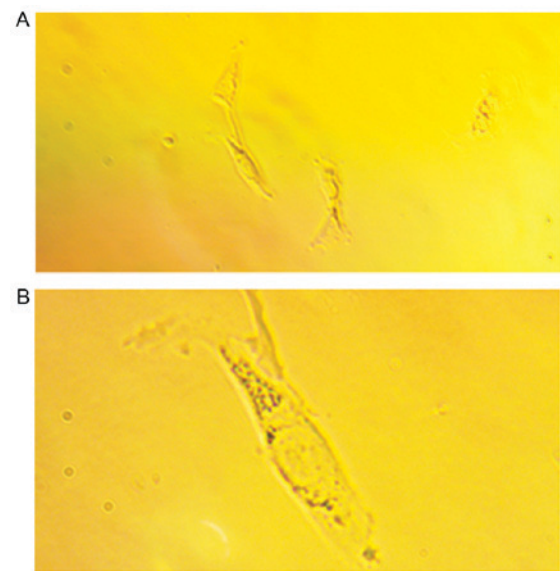

Figure 1. Detection of cell morphology under a microscope. (A) Cell clumps crowded with spindle cells were observed (magnification, x100). (B) Cells were spindle-shaped with one or more protuberances (magnification, x250). Cell nuclei were large with finely dispersed chromatin and 2-5 nucleoli.

Results

Cell morphology of atrial fibroblasts. At 3 days following incubation, cell clumps crowded with spindle cells were observed at x100 magnification (Fig. 1A). At x250 magnification, the atrial fibroblasts were spindle-shaped with one or more protuberances. Cell nuclei were large with finely dispersed chromatin and 2-5 nucleoli (Fig. 1B). In addition, following Masson trichrome staining, cytoplasmic granules such as ribosomes were stained in red and cell nuclei were in pale blue. Granular or cord-like blue components were observed, which represented the distribution of collagen in atrial fibroblasts (data not shown).

Identification of vimentin in atrial fibroblast. The expression of vimentin in atrial fibroblasts was detected by immunofluorescence assay. As demonstrated in Fig. 2, a large number of vimentin-positive cells (stained in green) were observed under confocal laser scanning microscopy. This result indicated that the atrial fibroblasts were successfully prepared.

Detection of cell proliferation following the different treatments. In the present study, cell proliferation was detected by MTS assay. To further identify the differences in cell proliferation, the growth curves of atrial fibroblasts following the different treatments based on cell counts on days 1, 3 and 5 were plotted and the slopes of the curves were calculated. The average slopes in the different groups were presented in Fig. 3. The slope values in the Glu, H_2O_2 and Glu+H_2O_2 groups were higher than those of the NC group, and there was a significant increase in the slope value in the H_2O_2 and Glu+H_2O_2 groups when compared with the NC group (P<0.05). The addition of apocynin inhibited cell proliferation, as demonstrated by the decrease in slope value in the Glu+Apo, H_2O_2+Apo and Glu+H_2O_2+Apo groups compared with the Glu, H_2O_2 and Glu+H_2O_2 groups, respectively
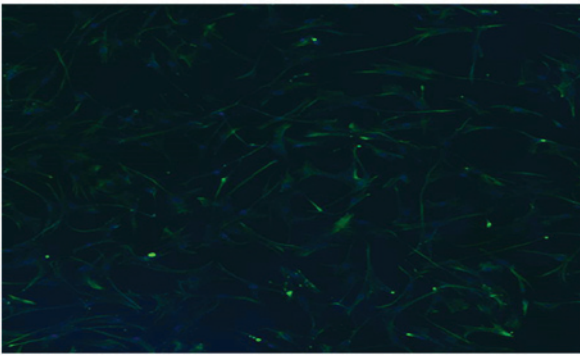
Figure 2. Identification of vimentin expression in atrial fibroblasts by immunofluorescence assay (magnification, x40). A total of 10 random fields were observed, a typical one is presented here. Vimentin-positive cells were stained in green.
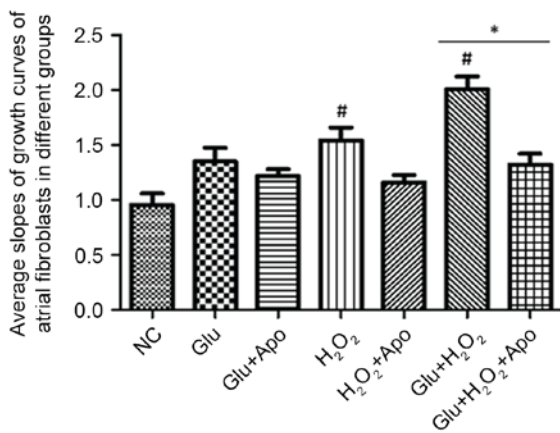

Figure 3. Effects of high glucose, H_2O_2 and apocynin on the slopes of growth curves of atrial fibroblasts. [#]$P<0.05$ vs. NC group; [*]$P<0.05$ as indicated. NC, normal control; Apo, apocynin; Glu group, cells were treated with 25 mM glucose; Glu+Apo group, cells were treated with 25 mM glucose and 100 µg/ml apocynin; H_2O_2 group, cells were treated with 100 nmol/l H_2O_2; H_2O_2+Apo group, cells were treated with 100 µg/ml apocynin and 100 nmol/l H_2O_2; Glu+H_2O_2 group, cells were treated with 25 mM glucose and 100 nmol/l H_2O_2; Glu+H_2O_2+Apo group, cells were treated with 25 mM glucose, 100 µg/ml apocynin and 100 nmol/l H_2O_2.

(Glu+H_2O_2+Apo vs. Glu+H_2O_2, $P<0.05$). In addition, no significant difference in slope value was observed when comparing the Glu+Apo, H_2O_2+Apo and Glu+H_2O_2+Apo groups with the NC group ($P>0.05$).

Detection of NADPH oxidase expression. Western blotting was performed to detect the expression of the NADPH oxidase subunits including Rac1 (regulatory subunit), p22phox and gp91phox (structural subunits), and the results were presented in Fig. 4. High glucose, H_2O_2 stimulation and a combination of high glucose and H_2O_2 treatment significantly increased the expression of Rac1 compared to the NC group ($P<0.05$) (Fig. 4A). However, addition of apocynin suppressed the elevated expression of Rac1 induced by high glucose, H_2O_2 stimulation and their combination, and a marked reduction was observed between Glu+Apo and Glu groups, and Glu+H_2O_2+Apo and Glu+H_2O_2 groups ($P<0.05$).

Additionally, high glucose and H_2O_2 stimulation did not affect the expression of the structural subunits (p22phox
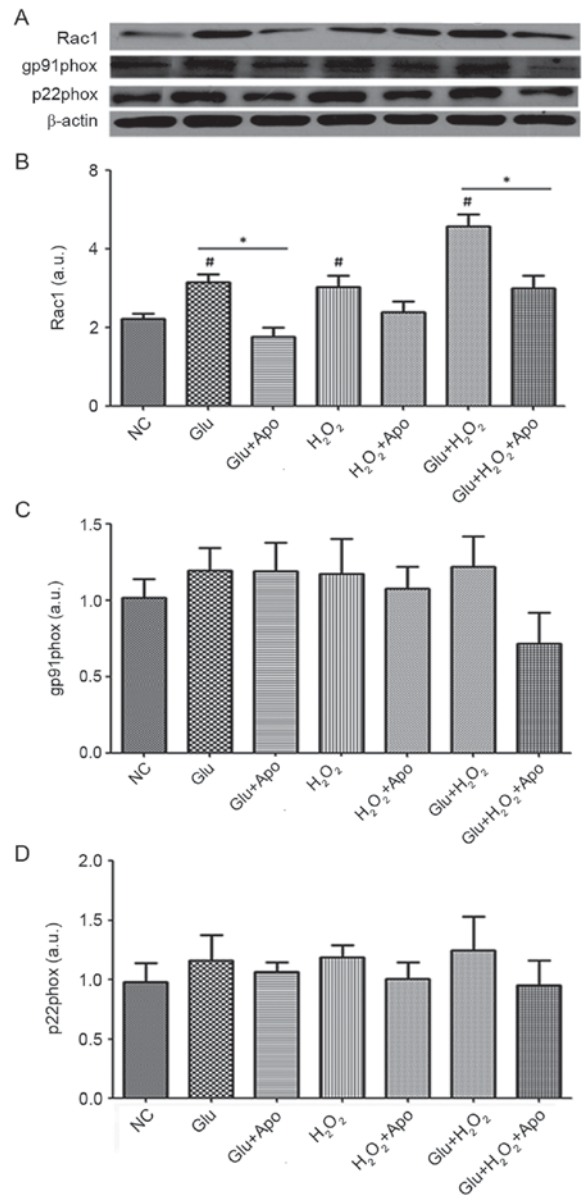

Figure 4. Effects of high glucose, H_2O_2 and apocynin on the expression of NAD(P)H oxidative subunits. (A) Representative Western blotting bands of Rac1, gp91phox and p22phox. (B) Quantitative expression levels of Rac1 protein. (C) Quantitative expression levels of gp91phox protein. (D) Quantitative expression levels of p22phox protein. [#]$P<0.05$ vs. NC group; [*]$P<0.05$ as indicated. NC, normal control; Apo, apocynin; Glu group, cells were treated with 25 mM glucose; Glu+Apo group, cells were treated with 25 mM glucose and 100 µg/ml apocynin; H_2O_2 group, cells were treated with 100 nmol/l H_2O_2; H_2O_2+Apo group, cells were treated with 100 µg/ml apocynin and 100 nmol/l H_2O_2; Glu+H_2O_2 group, cells were treated with 25 mM glucose and 100 nmol/l H_2O_2; Glu+H_2O_2+Apo group, cells were treated with 25 mM glucose, 100 µg/ml apocynin and 100 nmol/l H_2O_2; Rac1, Ras-related C3 botulinum toxin substrate 1 precursor; a.u., arbitrary units.

and gp91phox), and no significant differences in p22phox and gp91phox expression were observed when comparing Glu, H_2O_2 and Glu+H_2O_2 groups with the NC group (Fig. 4B and C). The addition of NADPH oxidase inhibitor apocynin did not significantly alter the expression of p22phox and gp91phox.

Detection of the expression and activity of key factors involved in mitogen-activated protein kinase (MAPK) signaling pathways. To reveal the ROS-mediated downstream events,
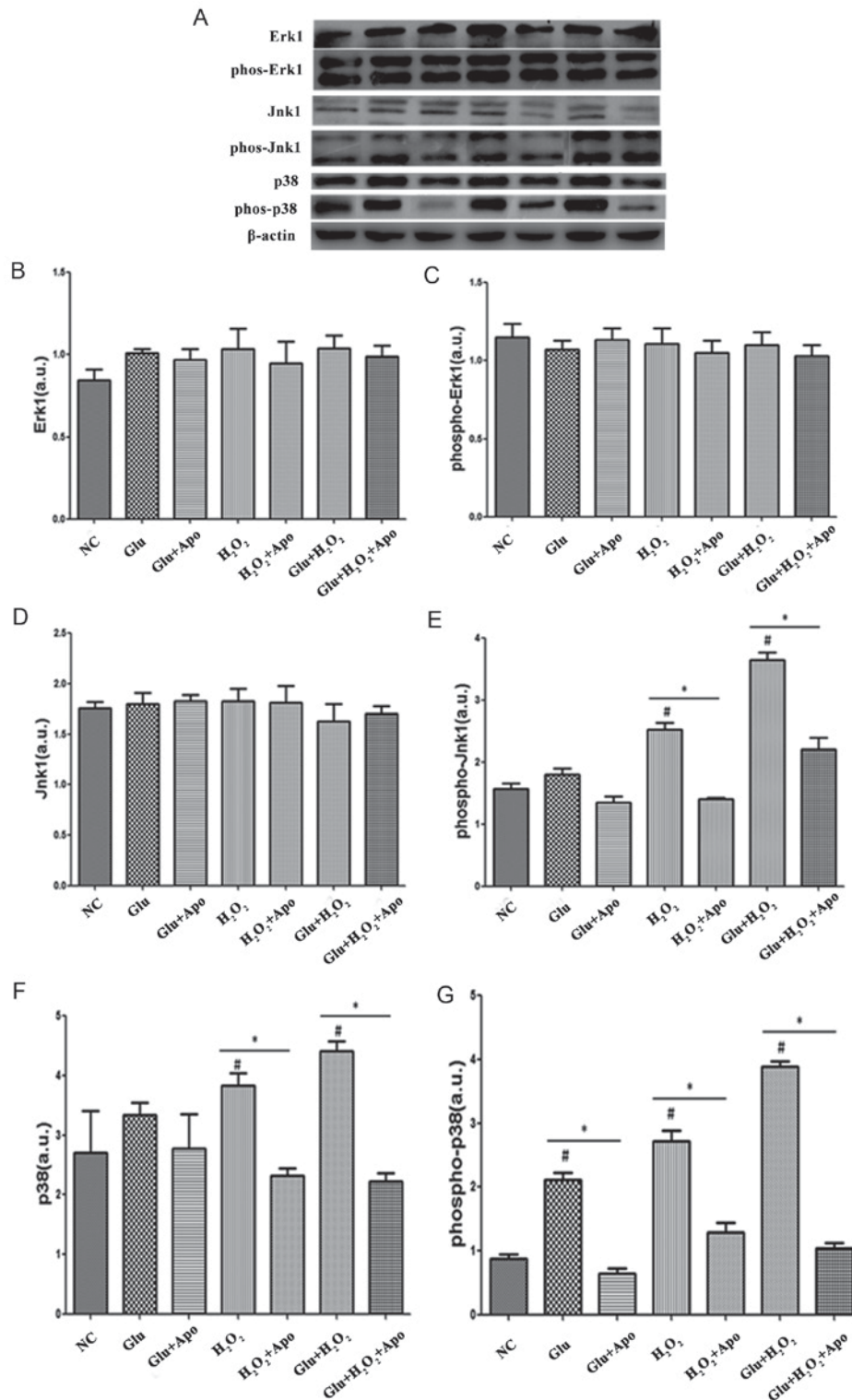
Figure 5. Effects of high glucose, H_2O_2 and apocynin on the expression of key factors involved in mitogen-activated protein kinase signaling pathways. (A) Representative western blotting bands of Erk1, phospho-Erk1, Jnk1, phospho-Jnk1, p38 and phospho-p38. (B) Quantitative expression levels of Erk1 protein. (C) Quantitative expression levels of phospho-Erk1 protein. (D) Quantitative expression levels of Jnk1 protein. (E) Quantitative expression levels of phospho-Jnk1 protein. (F) Quantitative expression levels of p38 protein. (G) Quantitative expression levels of phospho-p38 protein. [#]$P < 0.05$ vs. NC group; [*]$P < 0.05$, as indicated. Erk1, extracellular signal-regulated kinase 1; phospho/phos-, phosphorylated; Jnk1, c-Jun N-terminal kinase 1; NC, normal control; Apo, apocynin; Glu group, cells were treated with 25 mM glucose; Glu+Apo group, cells were treated with 25 mM glucose and 100 μg/ml apocynin; H_2O_2 group, cells were treated with 100 nmol/l H_2O_2; H_2O_2+Apo group, cells were treated with 100 μg/ml apocynin and 100 nmol/l H_2O_2; Glu+H_2O_2 group, cells were treated with 25 mM glucose and 100 nmol/l H_2O_2; Glu+H_2O_2+Apo group, cells were treated with 25 mM glucose, 100 μg/ml apocynin and 100 nmol/l H_2O_2; a.u., arbitrary units.

the present study also detected the expression of several key factors involved in MAPK signaling pathways and the results were shown in Fig. 5. When compared with the NC group, no

significant changes were observed in Erk1 and phospho-Erk1 expression following treatment with high glucose, H_2O_2 stimulation and their combination. The addition of apocynin did not
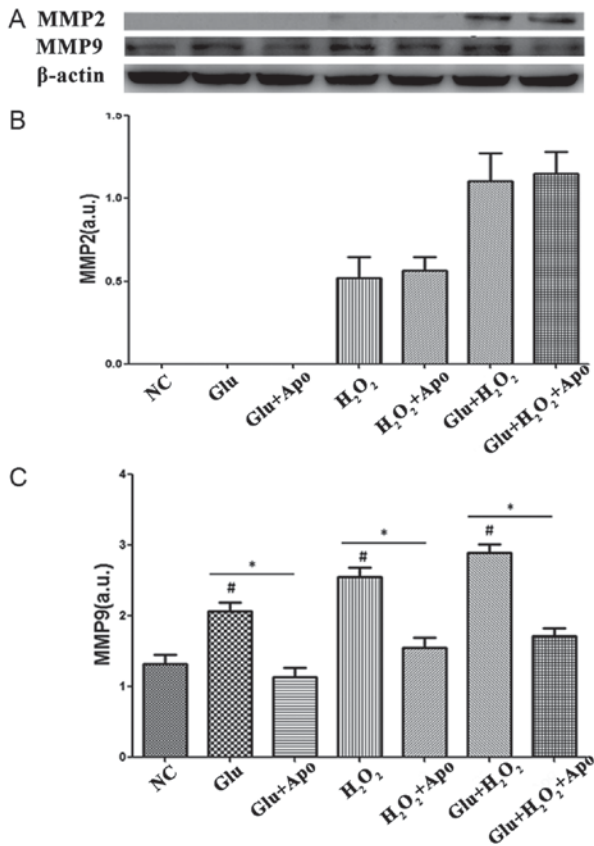
Figure 6. Effects of high glucose, H_2O_2 and apocynin on the expression of MMPs. (A) Representative Western blotting bands of MMP2 and MMP9. (B) Quantitative expression levels of MMP2 protein. (C) Quantitative expression levels of MMP9 protein. #$P<0.05$ vs. NC group; *$P<0.05$ as indicated. MMP, matrix metalloproteinase; NC, normal control; Apo, apocynin; Glu group, cells were treated with 25 mM glucose; Glu+Apo group, cells were treated with 25 mM glucose and 100 μg/ml apocynin; H_2O_2 group, cells were treated with 100 nmol/l H_2O_2; H_2O_2+Apo group, cells were treated with 100 μg/ml apocynin and 100 nmol/l H_2O_2; Glu+H_2O_2 group, cells were treated with 25 mM glucose and 100 nmol/l H_2O_2; Glu+H_2O_2+Apo group, cells were treated with 25 mM glucose, 100 μg/ml apocynin, and 100 nmol/l H_2O_2; a.u., arbitrary units.

significantly change the expression of Erk1 and phospho-Erk1 expression when compared with the corresponding treatment. Although there was no significant change in Jnk1 expression following high glucose and H_2O_2 treatment, the phospho-Jnk1 expression was significantly increased following H_2O_2 stimulation and the combination of high glucose and H_2O_2 stimulation ($P<0.05$). Additionally, the expression of phospho-Jnk1 was significantly reduced following the addition of apocynin when compared with the Glu+H_2O_2 and H_2O_2 groups ($P<0.05$). In addition, high glucose and H_2O_2 treatment induced an increase in p38 and phospho-p38 expression, and a significant difference was observed following H_2O_2 treatment and combined treatments for p38 expression, and for all treatments when analyzing phospho-p38 expression ($P<0.05$). The increased expression of p38 and phospho-p38 expression was significantly alleviated by the addition of apocynin ($P<0.05$).

Detection of the expression of MMPs. Western blotting was also performed to explore the expression of MMP2 and MMP9. As displayed in Fig. 6, the expression of MMP2 was undetectable in NC and Glu groups, and H_2O_2 stimulation induced a low expression of MMP2. The combined treatment of glucose and H_2O_2 induced an increased expression of MMP2, while the addition of apocynin did not significantly alter this increased expression of MMP2 induced by glucose and H_2O_2 stimulation. In addition, glucose, H_2O_2 stimulation and the combination treatment significantly increased the expression of MMP9 when compared with the NC group ($P<0.05$). Furthermore, the addition of apocynin markedly reduced the expression of MMP9 when compared with the corresponding group (Glu vs. Glu+Apo, H_2O_2 vs. H_2O_2+Apo, Glu+H_2O_2 vs. Glu+H_2O_2+Apo; $P<0.05$).

Discussion

Diabetes is a significant AF risk factor accounting for 10-25% of AF cases (24), while the underlying mechanisms associated with diabetes and AF remain under speculation. Increasing evidence has indicated that oxidative stress serves an important role in the pathogenesis of AF, and an increased level of ROS has been reported to be associated with AF development and maintenance (13,25). In addition, ROS production has been suggested to be involved in the AF pathophysiology in a diabetic rabbit model (26,27). The present study was performed to investigate the molecular mechanisms of increased ROS production in AF induced by diabetes as well as ROS-mediated downstream signaling pathways. The primary findings included: i) The atrial fibroblasts were successfully prepared from the atrium of the rabbits using enzyme digestion and differential adhesion; ii) high glucose and H_2O_2 stimulation promoted cell proliferation and the addition of apocynin inhibited this increase in atrial fibroblast proliferation induced by high glucose and H_2O_2 stimulation; iii) high glucose and H_2O_2 stimulation induced an increase in the expression of MMP9, NOXs subunits and key factors involved in the MAPK signaling pathways; iv) and the promoting effects of high glucose and H_2O_2 stimulation were attenuated by apocynin.

In the present study, atrial tissue samples were collected from the left atrium of rabbits and were digested by 2 enzymes (trypsin and collagenase II). Then, the atrial fibroblasts were obtained from differential adhesion. Following cell collection, the cultured cells were identified by cell morphology under a microscope and vimentin expression by immunofluorescence assay. The collected cells were spindle-shaped with one or more protuberances. Cell nuclei were large with finely dispersed chromatin and 2-5 nucleoli. Additionally, collagen was widely distributed in collected cells following Masson trichrome staining (data not shown). Vimentin, a type of intermediate filament protein, is a specific marker of fibroblasts and is widely used for identifying fibroblasts (28,29). Following the results in the present study, a large number of vimentin-positive cells were observed under confocal laser scanning microscope. All of these results indicated that atrial fibroblasts were successfully prepared.

Fibroblasts account for 75% of the total number of cardiac cells (30). As these cells are very small, fibroblasts only account for 10-15% of the total volume of the heart. The fibroblasts combined with the extracellular matrix constitute the cytoskeleton of heart (31). However, abnormal proliferation and differentiation of fibroblasts could induce fibrosis of cardiac tissues and dysfunction of cardiac function including

AF. A previous study indicated that oxidative stress is one of the activators for abnormal proliferation and differentiation of fibroblasts (32). In agreement with this, H_2O_2 stimulation induced an increase in the proliferation of atrial fibroblasts in the present study. In addition, hyperglycemia can enhance the glycation of proteins and lipids, leading to an increased generation of ROS (33,34). Thus, the imbalance between ROS production and scavenging through antioxidant mechanisms in diabetes results in increased oxidative stress. As presented in this study, a high glucose concentration also induced an increased proliferation of atrial fibroblasts, and the combination of high glucose and H_2O_2 stimulation presented markedly promotional effects on atrial fibroblast proliferation.

To reveal the underlying mechanism of increased ROS production and ROS-mediated downstream events, the present study detected the expression of several molecules including NOXs subunits, key molecules involved in MAPK signaling pathways as well as MMPs. NOXs are one of the primary sources for ROS and have been shown to be involved in various cardiovascular disorders through participating in redox signaling (35,36). Following the results in the present study, the expression of NOXs regulatory subunit Rac1 was significantly increased following high glucose and H_2O_2 stimulation, which was markedly attenuated by the addition of apocynin (the NOX inhibitor). Recently, apocynin has been demonstrated to prevent AF development and attenuate atrial remodeling in alloxan-induced diabetic rabbits (37). The present results indicated that ROS is excessively produced by NOXs in diabetes, contributing to the development of AF. A previous study indicated that diabetes enhanced oxidative stress, inflammatory responses in coronary cells as well the expression of MAPK signaling pathways (38). Several factors involved in the MAPK pathway are known to regulate the cellular response to stress, apoptosis and growth signals (36). As demonstrated in previous studies, phospho-p38 and JNK are activated by H_2O_2 in perfused rat hearts (39), and there is an increased expression of phospho-p38, phospho-JNK, ERK and phospho-ERK in diabetic rabbits (37). In the present study, it was demonstrated that a high level of glucose and H_2O_2 stimulation increased the expression of phospho-Jnk1, p38 and phospho-p38. These results indicated that the diabetes induced increase in ROS production in AF may be involved in MAPK signaling pathways, primarily in the signaling of phospho-JNK, p38 and phospho-p38. In addition, the expression of MMP2 and MMP9 were detected following different treatments. MMP9 expression was significantly increased following high glucose and H_2O_2 treatment, and the addition of the NOX inhibitor markedly attenuated the promotional effects on MMP9 expression induced by high glucose and H_2O_2 expression. However, MM2 expression did not markedly change following the different treatments. These results of the present study were consistent with a previous description, which reported that the expression of MMP9 increased during fibrillation of atrial tissue (40). These results indicated that the oxidative stress primarily present or induced by hyperglycemia would lead to the increased expression of MMP9, which may have contributed to the atrial structural remodeling during AF development.

In conclusion, the atrial fibroblasts were successfully prepared using enzyme digestion and differential adhesion in the present study. Hyperglycemia and oxidative stress induced an increase in atrial fibroblasts proliferation, leading to fibrosis of cardiac tissues and dysfunction of cardiac function, including AF. In addition, during AF development, excessive production of ROS was mainly derived from NOX activity and activation of ROS induced the expression of the MAPK signaling pathway, primarily including phospho-JNK, p38 and phospho-p38 and MMP9. These results provide the theoretical basis for the anti-oxidative therapy of atrial fibrillation caused by diabetes.

References

1. Čihák R, Haman L and Heinc P: Summary of the 2012 focused update of the ESC Guidelines for the management of atrial fibrillation: Prepared by the Czech Society of Cardiology. Cor Et Vasa 54: e341-e351, 2012.
2. Lip GY and Tse HF: Management of atrial fibrillation. Lancet 370: 604-618, 2007.
3. Wolf PA, Abbott RD and Kannel WB: Atrial fibrillation as an independent risk factor for stroke: The Framingham study. Stroke 22: 983-988, 1991.
4. Kalus JS, White CM, Caron MF, Coleman CI, Takata H and Kluger J: Indicators of atrial fibrillation risk in cardiac surgery patients on prophylactic amiodarone. Ann Thorac Surg 77: 1288-1292, 2004.
5. Fukahara K, Kotoh K, Doi T, Misaki T and Sumi S: Impact of preoperative atrial fibrillation on the late outcome of off-pump coronary artery bypass surgery. Eur J Cardiothorac Surg 38: 366-372, 2010.
6. Ad N, Henry L and Hunt S: The impact of surgical ablation in patients with low ejection fraction, heart failure, and atrial fibrillation. Eur J Cardiothorac Surg 40: 70-76, 2011.
7. Kanagaratnam P, Cherian A, Stanbridge RD, Glenville B, Severs NJ and Peters NS: Relationship between connexins and atrial activation during human atrial fibrillation. J Cardiovasc Electrophysiol 15: 206-216, 2004.
8. Patel C, Salahuddin M, Jones A, Patel A, Yan GX and Kowey PR: Atrial fibrillation: Pharmacological therapy. Curr Probl Cardiol 36: 87-120, 2011.
9. Sanguinetti MC and Bennett PB: Antiarrhythmic drug target choices and screening. Circ Res 93: 491-499, 2003.
10. Dudley SC Jr, Hoch NE, McCann LA, Honeycutt C, Diamandopoulos L, Fukai T, Harrison DG, Dikalov SI and Langberg J: Atrial fibrillation increases production of superoxide by the left atrium and left atrial appendage: Role of the NADPH and xanthine oxidases. Circulation 112: 1266-1273, 2005.
11. Neuman RB, Bloom HL, Shukrullah I, Darrow LA, Kleinbaum D, Jones DP and Dudley SC Jr: Oxidative stress markers are associated with persistent atrial fibrillation. Clin Chem 53: 1652-1657, 2007.
12. Chang JP, Chen MC, Liu WH, Yang CH, Chen CJ, Chen YL, Pan KL, Tsai TH and Chang HW: Atrial myocardial nox2 containing NADPH oxidase activity contribution to oxidative stress in mitral regurgitation: Potential mechanism for atrial remodeling. Cardiovasc Pathol 20: 99-106, 2011.

13. Kim YM, Guzik TJ, Zhang YH, Zhang MH, Kattach H, Ratnatunga C, Pillai R, Channon KM and Casadei B: A myocardial Nox2 containing NAD(P)H oxidase contributes to oxidative stress in human atrial fibrillation. Circ Res 97: 629-636, 2005.
14. Zhang J, Youn JY, Kim AY, Ramirez RJ, Gao L, Ngo D, Chen P, Scovotti J, Mahajan A and Cai H: NOX4-Dependent hydrogen peroxide overproduction in human atrial fibrillation and HL-1 atrial cells: Relationship to hypertension. Front Physiol 3: 140, 2012.
15. Babusíková E, Kaplán P, Lehotský J, Jesenák M and Dobrota D: Oxidative modification of rat cardiac mitochondrial membranes and myofibrils by hydroxyl radicals. Gen Physiol Biophys 23: 327-335, 2004.
16. Lai LP, Su MJ, Lin JL, Lin FY, Tsai CH, Chen YS, Huang SK, Tseng YZ and Lien WP: Down-regulation of L-type calcium channel and sarcoplasmic reticular Ca(2+)-ATPase mRNA in human atrial fibrillation without significant change in the mRNA of ryanodine receptor, calsequestrin and phospholamban: An insight into the mechanism of atrial electrical remodeling. J Am Coll Cardiol 33: 1231-1237, 1999.
17. Li GR and Nattel S: Properties of human atrial ICa at physiological temperatures and relevance to action potential. Am J Physiol 272: H227-H235, 1997.
18. Carnes CA, Chung MK, Nakayama T, Nakayama H, Baliga RS, Piao S, Kanderian A, Pavia S, Hamlin RL, McCarthy PM, *et al*: Ascorbate attenuates atrial pacing-induced peroxynitrite formation and electrical remodeling and decreases the incidence of postoperative atrial fibrillation. Circ Res 89: E32-E38, 2001.
19. Anderson EJ, Kypson AP, Rodriguez E, Anderson CA, Lehr EJ and Neufer PD: Substrate-specific derangements in mitochondrial metabolism and redox balance in the atrium of the type 2 diabetic human heart. J Am Coll Cardiol 54: 1891-1898, 2009.
20. Nichols GA, Reinier K and Chugh SS: Independent contribution of diabetes to increased prevalence and incidence of atrial fibrillation. Diabetes Care 32: 1851-1856, 2009.
21. Goudis CA, Korantzopoulos P, Ntalas IV, Kallergis EM, Liu T and Ketikoglou DG: Diabetes mellitus and atrial fibrillation: Pathophysiological mechanisms and potential upstream therapies. Int J Cardiol 184: 617-622, 2015.
22. van Heerebeek L, Hamdani N, Handoko ML, Falcao-Pires I, Musters RJ, Kupreishvili K, Ijsselmuiden AJ, Schalkwijk CG, Bronzwaer JG, Diamant M, *et al*: Diastolic stiffness of the failing diabetic heart: Importance of fibrosis, advanced glycation end products, and myocyte resting tension. Circulation 117: 43-51, 2008.
23. Zhang Q, Liu T, Ng CY and Li G: diabetes mellitus and atrial remodeling: Mechanisms and potential upstream therapies. Cardiovasc Ther 32: 233-241, 2014.
24. Mohammad MR, Hashemzadeh M and Jamal MM: Diabetes mellitus is a strong, independent risk for atrial fibrillation and flutter in addition to other cardiovascular disease. Int J Cardiol 105: 315-318, 2005.
25. Korantzopoulos P, Kolettis TM, Galaris D and Goudevenos JA: The role of oxidative stress in the pathogenesis and perpetuation of atrial fibrillation. Int J Cardiol 115: 135-143, 2007.
26. Liu T, Zhao H, Li J, Korantzopoulos P and Li G: Rosiglitazone attenuates atrial structural remodeling and atrial fibrillation promotion in alloxan-induced diabetic rabbits. Cardiovasc Ther 32: 178-183, 2014.

27. Fu H, Li G, Liu C, Li J, Wang X, Cheng L and Liu T: Probucol prevents atrial remodeling by inhibiting oxidative stress and TNF-α/NF-κB/TGF-β signal transduction pathway in alloxan-induced diabetic rabbits. J Cardiovasc Electrophysiol 26: 211-222, 2015.
28. Krenning G, Zeisberg EM and Kalluri R: The origin of fibroblasts and mechanism of cardiac fibrosis. J Cell Physiol 225: 631-637, 2010.
29. Ieda M, Fu JD, Delgado-Olguin P, Vedantham V, Hayashi Y, Bruneau BG and Srivastava D: Direct reprogramming of fibroblasts into functional cardiomyocytes by defined factors. Cell 142: 375-386, 2010.
30. Shiraishi I, Takamatsu T, Minamikawa T, Onouchi Z and Fujita S: Quantitative histological analysis of the human sinoatrial node during growth and aging. Circulation 85: 2176-2184, 1992.
31. Shiraishi I, Takamatsu T, Minamikawa T and Fujita S: 3-D observation of actin filaments during cardiac myofibrinogenesis in chick embryo using a confocal laser scanning microscope. Anat Embryol (Berl) 185: 401-408, 1992.
32. Burstein B and Nattel S: Atrial fibrosis: Mechanisms and clinical relevance in atrial fibrillation. J Am Coll Cardiol 51: 802-809, 2008.
33. Sayed AA, Khalifa M and Abd el-Latif FF: Fenugreek attenuation of diabetic nephropathy in alloxan-diabetic rats: Attenuation of diabetic nephropathy in rats. J Physiol Biochem 68: 263-269, 2012.
34. Aljofan M and Ding H: High glucose increases expression of cyclooxygenase-2, increases oxidative stress and decreases the generation of nitric oxide in mouse microvessel endothelial cells. J Cell Physiol 222: 669-675, 2010.
35. Li JM, Gall NP, Grieve DJ, Chen M and Shah AM: Activation of NADPH oxidase during progression of cardiac hypertrophy to failure. Hypertension 40: 477-484, 2002.
36. Griendling KK, Sorescu D and Ushio-Fukai M: NAD(P)H oxidase: Role in cardiovascular biology and disease. Circ Res 86: 494-501, 2000.
37. Qiu J, Zhao J, Li J, Liang X, Yang Y, Zhang Z, Zhang X, Fu H, Korantzopoulos P, Liu T and Li G: NADPH oxidase inhibitor apocynin prevents atrial remodeling in alloxan-induced diabetic rabbits. Int J Cardiol 221: 812-819, 2016.
38. Zhang L, Zalewski A, Liu Y, Mazurek T, Cowan S, Martin JL, Hofmann SM, Vlassara H and Shi Y: Diabetes-induced oxidative stress and low-grade inflammation in porcine coronary arteries. Circulation 108: 472-478, 2003.
39. Clerk A, Fuller SJ, Michael A and Sugden PH: Stimulation of 'stress-regulated' mitogen-activated protein kinases (stress-activated protein kinases/c-Jun N-terminal kinases and p38-mitogen-activated protein kinases) in perfused rat hearts by oxidative and other stresses. J Biol Chem 273: 7228-7234, 1998.
40. Nakano Y, Niida S, Dote K, Takenaka S, Hirao H, Miura F, Ishida M, Shingu T, Sueda T, Yoshizumi M and Chayama K: Matrix metalloproteinase-9 contributes to human atrial remodeling during atrial fibrillation. J Am Coll Cardiol 43: 818-825, 2004.